Experimental and DFT studies on the structural and optical properties of chitosan/polyvinyle pyrrolidone/ZnS nano composites

A. M. Abdelghany (a.m_abdelghany@yahoo.com)
National Research Centre https://orcid.org/0000-0001-8953-0056
M.A. Aboelwafa
Mansoura University Faculty of Science
M.S. Meikhail
Mansoura University Faculty of Science
A Oraby
Mansoura University Faculty of Science

Research Article

Keywords: Chitosan (CS), Polyvinyl pyrrolidone (PVP), Zinc sulfide (ZnS), FTIR, UV/Vis, Optical spectroscopy, DFT

Posted Date: April 22nd, 2021

DOI: https://doi.org/10.21203/rs.3.rs-331123/v1

Abstract

Chitosan/ Polyvinyl pyrrolidone (CS/PVP) semi-natural polymeric blend involving gradient concentrations of ZnS nanoparticles (ZnS-NPS) was prepared via a simple casting method. In conjunction with computational density functional theory approaches (DFT), prepared samples were characterized by UV/Vis spectrophotometric studies and Fourier transform infrared measurements (FTIR) to take into account a detailed description of the different reaction mechanisms within the polymeric matrices. To conduct all calculations, the Becke three-parameter hybrid functional (B3LYP) correlation function used with the electron core potential basis set LANL2DZ was used. A detailed study for different reaction regimes was studied and reaction via Oxygen was observed to be preferred and compatible with that of the experimental data. UV/vis. Absorption experimental data were used to calculate the optical energy gap using the Mott-Davis equation and observed data was found to follow an indirect transition route.

Introduction

Polymer blending is an enticing route for creating new polymeric materials with customized properties that are preferable to that of each polymer product. Polymer blend (PB) is a combination of at least two polymers or copolymers mixed to form a new substance with specific physical characteristics, in which the content of the ingredient is greater than2 wt.%. This behavior depends on the solubilities between the components of the polymer mixture. The blending of two or more polymers become very essential to improve production efficiency by manufacturing products with a complete range of desired properties, improving specific properties, mixing with a more rigid and heat-resistant resin can result in better modulus and dimensional stability but provide means for the regeneration of industrial and/or municipal waste plastic [1–3].

The second most frequent biopolymer of Polysaccharides of biological origin is chitosan present in nature (after cellulose). It was derived from shells of shrimp, krill crab, lobster, and prawn and can be synthesized usage of chitin as a raw resource through a deacetylase reaction [4]. Chitin contains good chemical composition and strong membrane-forming properties and soluble in water solutions with low acidity, renewable, and non-toxic. This is a perfect biodegradable that can be deposited underground without disturbing the normal circulation of the environment. Due to the extreme properties of chitosan such as antimicrobial activity, biocompatibility, and non-toxicity which is widely used in wound healing and dressing. The drawbacks of chitin include the ease of degradation by ultraviolet radiation, the difficulty of rotating lead to a lack of wet strength results, have little water solubility, and absence of processability due to low heat resistance. Chitosan was used in various areas of use such as product packaging, isolation or purification, biomedical and edible materials [5].

Polyvinyl pyrrolidone (PVP) is an amorphous, synthetic polymer and has high Tg values up to 170C due appearance of a solid pyrrolidone group, which is heavy with the drawing group and is known to form separate complexes with other polymers. It exhibits high wetting properties and shapes films quickly in the solution. This works nicely as a paint or a coating additive. PVP as just a water-soluble polymer

provides positive effects on safety, viscosity, absorbency, solubilization, and condensation, the most important characteristics of which are superior solubility and biological performance. Also, PVP possesses low toxicity and is used in a wide range of fields, including health-related domains, cosmetics, and medical, food packaging. However, issues related to the stable yet delicate nature of the PVP and its loss of robustness have led to difficulties in production. Due to its extremely low cytotoxicity, it is widely used in medicine. The other uses are in biological and pharmaceutical technology and electrochemical instruments (batteries, displays) [6–8].

Zinc sulfide nanoparticles (ZnS-NPS) are important group II-IV semiconductors with unique properties, which can be found in one of the two structural forms cubic sphalerite or hexagonal wurtzite. The properties of ZnS are highly dependent on their size, structural form, and morphology. This non-toxic material, which is chemically more stable than other semiconductors, is characterized by a wide band-gap energy of ~ 3.7 eV. Because of these properties, ZnS nanoparticles can be used in both biomedical and optoelectronic applications, such as biosensors, bio-composites, cell tagging, light-emitting diode (LED), and apply these technologies to other fields, such as optoelectronics, marking, monitoring agents, information collection, optics, fluorescent probes, and drug distribution [9–12].

The presented work aims to effect gradually increased zinc sulfide nanoparticles on the structure and physical properties of a semi-natural polymer blend comprising 80% poly vinyl pyrrolidone and 20% of chitosan.

2. Detailed Experimental Work

2.1. Materials used

Chitosan (Cs) with a deacetylation degree of 86% extra pure was obtained from the exporter lab chemicals Co. (Alpha Chemika, India). Polyvinyl pyrrolidone (PVP) (MW 40.000), (purity > 99%) was obtained from (Bio Basic Canada INC.). Zinc sulfide nanoparticles (ZnS-NPS) (MW 97.43 g/mol) were supplied by European Economic Community (EEC).

2.2. Sample Preparation and characterization

Studied samples were synthesized in the form of thin membrane films using the traditional solvent casting and evaporation route. A calculated amount of the Cs was dissolved through vigorous stirring in (50 mL) of 2% aqueous solution of acetic acid and mixed with a specific amount of PVP and stirred for 60 min. Then mixed solution dropped on clean Petri dishes and dried at 50°C for 24h. PVP/CS (80/20) blend was prepared with various loading concentrations of zinc sulfide nanoparticles (ZnS-NPS) as shown in Table (1). All samples were prepared via the same route and dropped on clean Petri dishes and dried at 50°C.

Table (1): Samples with different amounts of ZnS-NPS.

Sample	(PVP/CS) (wt%)	ZnS (10^{-4})
S_0	80:20	0
S_1	80:20	2.5
S_2	80:20	5
S_3	80:20	10
S_4	80:20	20

The FTIR optical absorption spectra were recorded under the spectral spectrum of 4000 – 400 cm^{-1} using a single beam Nicolet is 10 spectrometers, absorption mode with 32 scans and a resolution of 2 cm^{-1} to analyze to recognize vibration bands associated with major chemical groups, detect the molecular structure and intermolecular interaction between polymers. The optical properties of the samples were detected utilizing UV\Vis. spectrophotometer (V-570 UV/Vis–NIR, JASCO Corp) in the 200–1100 nm wavelength range at room temperature. Calculations were achieved using the Gaussian 09 software within the application of DFT. Density functional calculations have been employed to ensure reaction mechanisms through an agreement between the experimental measured and theoretical calculated data. Both expected structures have been enhanced using Becke, 3-parameter Lee–Yang–Parr (B3LYP).

3. Result And Discussion

3.1. Fourier transforms infrared analysis (FTIR)

FT-IR spectroscopy is a very powerful technique to recognize vibration bands associated with major chemical groups, detect the molecular structure which means characterizing the assignment of bands for each sample and inter-molecular interaction between polymers. Figures (1) shows FT-IR absorbance spectra in the range 4000 – 500 $cm^{-1}$of pure PVP, CS, and CS/PVP composites films at room temperature are registered. The positions of the FTIR absorption band and their functions are shown in table (2).

For pure PVP; the spectra show broadband at about 3451 cm^{-1} is delegated the hydroxyl group (OH) stretching vibration because PVP is hygroscopic [13–15]. In conjunction, four overlapping signals can be applied to the (CH) stretching modes: symmetrical CH_2 stretching at approximately 2885 cm^{-1}, asymmetrical CH_2 stretching at approximately 2943 cm^{-1} [16–17], peaks at 1446 cm^{-1} and 1370 cm^{-1} also referring to the CH deformation modes of the CH_2 group [18]. The stretching vibration near 1662 cm^{-1} can be due to C = O in the pyrrolidone group [14, 19–20]. Besides, bending vibrations at 1291 cm^{-1}, which are connected to the C–N of the pyrrolidone structure, may be identified. It is remembered that PVP is just a bi-substituted amide, characteristic absorption of amines at about 3400–3500 cm^{-1} have not been found [13, 21]. The band at 750 cm^{-1} corresponds to C–C chain. The bands at 655 cm^{-1} and 567

cm^{-1} correspond to N–C = O [15]. For pure CS; the hallmark of absorption bands at 3424 cm^{-1} assign to (O ▯ H) overlapped with (N ▯ H) stretching vibration [22, 4],Also, the characteristic band at 2880 cm^{-1} assigned to (C ▯ H) stretching [22–24], Also, the at 1653 cm^{-1} assigned to C = O stretching (amide II) O = C-NHR. The peak at 1574 cm^{-1} is assigned for (NH) bending (amide I) (NH2) [25]. The results of the coupling of(N-H) angular deformation and (C-N) axial stretching at 1426 cm^{-1} and 1382 cm^{-1} [26], the absorption bands at 1160 cm^{-1} assign to (C-O-C bridge) anti-symmetric stretching [23], the peaks at 1076 cm^{-1}, 1035 cm^{-1}, and 665 cm^{-1} are characteristic of its saccharide structure (skeletal vibrations involving the C-O stretching) [22–24]. For the PVP/CS blend; absorption spectra were seen at 3451 cm^{-1}, attributed to the (-OH) and (–NH) groups. Chitosan (–OH) and (–NH) absorption spectra groups at approximately 3424 cm^{-1} were observed to be drifting towards a higher frequency region with the inclusion of PVP to form a blended polymer. The prominent peaks at 2943 $cm^{-1}$and 2884 cm^{-1} were assigned to the methylene group (CH_2) in the PVP and CS of asymmetrical and symmetrical stretching vibrations. The position of the characteristic band of chitosan at 1633 cm^{-1} is shifted in blends to a higher frequency (1662 cm^{-1} for the blend with composition 80/20). It indicates the presence of hydrogen bonding between PVP and CS. Chitosan, a hydrogen sender, forms a hydrogen bond with the PVP carbonyl group.

Pyrrolidone rings in PVP contain a proton that embraces carbonyl moiety, which chitosan introduces as side groups hydroxyl and amino. Hydrogen bonding interactions between these two chemical fractions can also take place in a mixture of CS and PVP. The existence of hydrogen bonds between two specific macromolecules competes with the formation of hydrogen bonds between molecules of the same polymer. The peak at 1430 cm^{-1} is the result of the coupling of N-H angular deformation and C-N axial stretching. the peak at 1291 cm^{-1} was due to C–N stretching vibration and this confirmed the presence of amine group in pure in the membrane matrix. The peaks at 1076 cm^{-1} and 1035 cm^{-1} (skeletal vibrations involving the C–O stretching) are characteristic of its saccharide framework.

Table (2): Allocations of the FTIR characterization bands of the pure PVP and pure CS.

PVP		CS	
Wavenumber (cm^{-1})	Assignment	Wavenumber (cm^{-1})	Assignment
3451	stretching (O-H)	3424	(O-H) overlap with (N-H) Stretching
2943	(CH_2) asymmetric stretching	2880	(CH) symmetric stretching
2885	(CH_2) symmetric stretching	1653	C = O stretching (amide II) O = C-NHR
1446 and 1370	CH deformation modes from the CH_2 group	1574	NH bending (amide I)
1662	(C = O) symmetric stretching	1426,1382	coupling N-H angular deformation and of C-N axial stretching
1291	symmetric stretching (C ▯ N)	1160	(C-O-C bridge) anti-symmetric stretching
750	C-C	1076, 1035, 665	stretching (C-O) and specifying to saccharide structure Stretching
655 and 567	N-C = O		

Figure (2) indicate FTIR absorption in the region of 4000-500 cm^{-1} for comparing the spectra of a blend (PVP/CS) when blending with various concentration of zinc sulfide nanoparticles (ZnS-NPS) reveal that the spectral changes appear as a result of ZnS blending and exhibit the characteristic bands in the table (3). First, the stretching vibration of hydroxyl groups (O-H) locates at 3400-3500 cm^{-1} of (PVP/CS) and appears a sharp band after merging different concentration of ZnS-NPs with a blend that becomes broad is sample S2 and then splits with increasing concentration of ZnS-NPS up to (0.1%). Second, the band at 1662 cm^{-1} decreases in intensity, and the width of the band increase with an increase in the concentration of ZnS-NPs which demonstrates the complexation between ZnS-NPs and (PVP/CS) polymer blend by a coordinate bond. Third, there was a strong shift in severity with a rise in the content of ZnS doping. The peaks at 1434 cm^{-1} and 1283 cm^{-1} become broad and decrease in intensity with increasing the concentration of ZnS-NPS up to (0.025%).

Table (3) Assignments of the FT-IR characterization bands of the blend (PVP/CS) and PVP/CS/ZnS

PVP/CS		PVP/CS/ZnS	
Wavenumber (cm^{-1})	Assignment	Wavenumber (cm^{-1})	Assignment
3451	stretching (O-H)	3462	stretching (O-H)
2943	asymmetric stretching (CH_2)	2945	asymmetric stretching (CH_2)
2884	symmetric stretching (CH_2)	2896	symmetric stretching (CH_2)
1662	symmetric stretching (C = O)	1662	(C = O) Symmetric stretching
1430	coupling of (N-H) angular deformation and (C-N) axial stretching	1434	coupling of (N-H) angular deformation and (C-N) axial stretching
1291	stretching vibration (C–N)		
1076,1035,655	C-O stretching and specifying to saccharide structure Stretching		

3.2. Density function theory (DFT)

The theoretical methodology is used to describe the framework of connection between polymeric matrices and to calculate the degree of agreement with experimental evidence for complicated interactions between components (Polyvinyl pyrrolidone and chitosan).

All measurements were calculated using Gaussian 09 software within the DFT system. A blend of (PVP/CS) and blend-ZnS system were designed using the Becke three-parameter hybrid functional (B3LYP) correlation function used with the electron core potential basis collection LANL2DZ.

Figure (3) reveals an optimized 3D structure for Polyvinyl pyrrolidone monomer in combination with both experimental FT-IR and calculated infrared spectra that show a new band which obtained in the experimental data is not obtained in the theoretical data hence it's maybe that the PVP is hygroscopic.

Table (4) present the DFT and experimental FT-IR spectral band position of PVP polymer.

Table (4): DFT and experimental FT-IR spectral data of PVP monomer

Experimental Peak location (cm^{-1})	Theoretical Peak location (cm^{-1})	Band Assignment
3451		(O-H) stretching
2943		asymmetric stretching (CH_2)
2885		symmetric stretching (CH_2)
1446 and 1370	1456 and 1400	CH deformation modes from the CH_2 group
1662	1664	(C=O) symmetric stretching
1291	1300	(C N) symmetric stretching
750	740	correspond to C-C
655 and 567	652 and 574	correspond to N-C=O

Figure (4) reveals an optimized 3D structure for chitosan monomer in combination with both experimental FT-IR and calculated infrared spectra.

Table (5) present the DFT and experimental FT-IR spectral band position of Chitosan polymer.

Table (5): DFT and experimental FT-IR spectral data of Chitosan monomer.

Experimental Peak location (cm^{-1})	Theoretical Peak location (cm^{-1})	Band Assignment
3424	3547	(O-H) overlap with (N-H) Stretching
2880		(CH) symmetric stretching
1653	1669	C=O stretching (amide II) O=C-NHR
1574		NH bending (amide I)
1426,1382	1452,1370	coupling of N-H angular deformation and C-N axial stretching
1160	1203	(C-O-C bridge) anti-symmetric stretching
1076,1035,665	1070,1043 and 595	stretching (C-O) and specifying to saccharide structure Stretching

Figure (5) show two separate probability of contact between PVP and CS and also shows the optimized structure arising from DFT. while experimental data of 80/20 PVP/Cs polymer blend and theoretical FTIR of the two probabilities of interaction using DFT calculations

Table (6) DFT and experimental FT-IR spectral data of PVP/Chitosan polymer blend.

Experimental Peak Position (cm^{-1})	Theoretical Peak Position (cm^{-1})	Band Assignment
3451	3458	(O-H) stretching
2943	3064	asymmetric stretching (CH_2)
2884	2990	symmetric stretching (CH_2)
1662	1663	symmetric stretching (C=O)
1430	1429	coupling of N-H angular deformation and C-N axial stretching
1291	1297	C–N stretching vibration
1076, 655	1071, 658	C-O stretching and specifying to saccharide structure Stretching

Figure (7) shows a schematic diagram of the 2D and 3D interaction mechanism probabilities between PVP/CS poly-blend and ZnS-NP.

Table (7) DFT and experimental FT-IR spectral data of PVP/CS/ZnS.

Experimental peak location(cm^{-1})	Theoretic peak location (cm-1)	Band Assignment
3462	3500	(O-H) stretching
2945	2930	asymmetric stretching (CH_2)
1662	1535	symmetric stretching (C=O)
1434	1440	coupling of N-H angular deformation and C-N axial stretching
1291	1315	C-N stretching vibration
1076	1078	saccharide structure stretching

3.3. Optical properties in ultraviolet/visible regions

A valuable method for sample analysis is ultraviolet-visible (UV/Vis.) spectroscopy. it provides an understanding of the importance of optical parameters, including bandgap energy ( ) and the absorption of light energies by polymer composites in UV and visible areas, which include the move of electrons from the ground state (σ, π, and orbital) to higher energy states described by molecular orbitals [27]. The result of absorption studies with UV/Vis. spectrophotometer in the wavelength 200-1100 nm carried out on pure blend and samples contains ZnS-NPS as illustrated in figure (9). The samples display only one absorption peak at approximately 230 nm with no other peak before the end of the measurements. This

can be due to the translucent existence of both the PVP and the CS, and the previously reported data [28] referred to the absorption band at approximately 225 nm as a result of the π → π* electronic transition that comes from unsaturated bonds, mainly C=O bond which identified by in FT-IR at about 1662 cm^{-1}.

Figure (9) reveals the absorption peaks of samples (S1, S2, S3, and S4) show the onest absorption peaks and increase in intensity with increasing concentration of ZnS-NPs this may be due to interaction between the two (PVP/CS) blend and ZnS-NPs, and the value of wavelength are slightly increased.

Identification of the optical band ga*p (Eg)*

The optical technique can analyze optically induced transitions and provide data on the bonding structure of organic compounds and the energy gap among crystalline and non-crystalline samples. Semiconductors are usually categorized into two kinds: (a) direct band spacing and (b) indirect band spacing. In the direct band spacing, the head of the valence band and the rest of the conduction band have the same momentum magnitude. If the bottom of the conduction band does not equate to zero crystal momentum, it is called the indirect band spacing. From the optical absorption spectra using the Beer-Lambert relationship (1), the absorption coefficient can be calculated as follows:

$$\alpha(\nu) = 2.303\left(\frac{A}{L}\right) \qquad (1)$$

where A is the absorbance, log (I_0/I) is defined where I_0 and I are the strength of the incident and transmitted beams, respectively and L is the film thickness in cm. Analysis of the spectral dependence of absorption at the absorption edge can determine the optical bandgap. Concerning optical transitions resulting from energy photons hn>Eg, the present optical data can be analyzed for near-edge optical absorption according to the following relationship (2).

$$\alpha(\nu)h\nu = \beta\,(h\nu - E_g)^r \qquad (2)$$

Where Eg is the magnitude of the optical energy gap, is the energy of the incident photons, and r is the force that characterizes the transformation phase in K-space. In specific, depending on the type of electron transitions responsible for optical absorption, r will take the values 1, 2, 3, ½, and 3/2. It is valid that the value of r is 2 in the case of a direct electronic transition over a direct energy gap in K space and ½ in the case of an indirect electronic transition over an indirect energy gap. The factor β is based on the probability of transformation and can be assumed to be stable within the optical frequency spectrum. The usual procedure for calculating the value of Eg involves plotting $(\alpha h\nu)^r$ against (hv). The dependence of $(\alpha h\nu)^r$ and photon energy (hv) was plotted for the films analyzed using various values of r (1/2, 2). Close to the absorption edge for the present experimental results, the plots of $(\alpha\, h\nu)^{1/2}$ and $(\alpha\, h\nu)^2$ vs. (hv) of the absorption edge produce a linear fit over a broader range of hn, as seen in Figure (10).

The Eg values of the films were calculated from the linear part of these curves, and given in table (8). From this table, in general, the value of value Eg decreases with increasing ZnS-NPs content.

Table (8): The variation of optical properties for PVP/CS blended with different concentrations of ZnS-NPs.

Sample	ZnS con. (10^{-4})	Absorption edge (λg) (nm)	$E_{optical}$	E_{direct}	$E_{indirect}$
S0	0.0	262.944	4.7149	4.135	4.770
S1	2.5	244.739	5.066	4.684	5.077
S2	5.0	250.742	4.945	4.597	5.054
S3	10	262.944	4.716	4.169	4.786
S4	20	250.549	4.950	4.477	4.913

Conclusion

Infrared spectrophotometric measurements by Fourier transform (FTIR) shows the maintenance of pure PVP, CS, and (PVP/CS) polymer blend characteristic bands in conjunction with computational density functional theory approaches (DFT) and does not show the existence of any new peaks. The proposed potential reaction mechanisms are performed by computational data and give the percentage compatibility between experimental and computed spectral data through function (B3LYP) and basis set LANL2DZ.

References

1. Ahmed, R.M.: Optical study on poly (methylmethacrylate)/poly (vinyl acetate) blends. Int. J. Photoenergy **41**, 1–7 (2009)
2. Isayev, A.I.: Encyclopedia of polymer blends, JAWS, 1(2010)
3. Utracki, L.A., Wilkie, C.A.: Polymer blends handbook second edition, J. Springer, 2014
4. Yeh, J.T., Chen, C.L., Huang, K.S., Nien, Y.H., Chen, J.L., Huang, P.Z.: Synthesis, characterization, and application of PVP/chitosan blended polymers. J. Appl. Polym. Sci. **101**, 885–891 (2006)
5. Yun, Y.H., Youn, H.G., Shin, J.N., Yoon, S.D.: Preparation of functional chitosan-based nanocomposite films containing ZnS nanoparticles. Int. J. Biol. Macromol. **104**, 1150–1157 (2017)
6. Karpuraranjith, M., Thambidurai, S.: Chitosan/zinc oxide-polyvinylpyrrolidone (CS/ZnO-PVP) nanocomposite for better thermal and antibacterial activity. Int. J. Biol. Macromol. **104**, 1753–1761 (2017)
7. Poonguzhali, R., Basha, S.K., Kumari, V.S.: Synthesis and characterization of chitosan/poly (vinylpyrrolidone) biocomposite for biomedical application. Int. J. Biol. Macromol **105**, 111–120

(2017)

8. Seabra, A.B., Oliveira, M.G.: Poly (vinyl alcohol) and poly (vinyl pyrrolidone) blended films for local nitric oxide release. Biomater. Res. **25**, 3773–3782 (2004)
9. Ali, H., Karim, S., Rafiq, M.A., Maaz, K., Rahman, A., Nisar, A., Ahmad, M.: Electrical conduction mechanism in ZnS nanoparticles. J. Alloys Compd. **612**, 64–68 (2014)
10. Dutta, K., Manna, S.: and S.K. De., Optical and electrical characterizations of ZnS nanoparticles embedded in conducting polymer. J. Synth. Met. **159**, 315–319 (2009)
11. Tiwari, A., Dhobleb., S.J.: Stabilization of ZnS nanoparticles by polymeric matrices: syntheses, optical properties and recent applications. RSC Adv. **6**, 64400–64420 (2016)
12. Soltani, N., Saion, E., Hussein, M.Z.: Influence of the polyvinyl pyrrolidone concentration on particle size and dispersion of ZnS nanoparticles synthesized by microwave irradiation. Int. J. Mol. Sci. **13**, 12412–12427 (2012)
13. Abdelghany, A.M., Abdelrazek, E.M., Rashad, D.S.: Impact of in-situ preparation of CdS Filled PVP Nano- composite. Spectrochimica **130**, 302–308 (2014)
14. Marsano, E., Vicini, S., Skopinska, J., Wisniewski, M., Sionkowska, A.: Chitosan and poly (vinyl pyrrolidone): compatibility and miscibility of blends, Macromol. Symp., 218(2004) 251–260
15. Basha, M.A.F.: Magnetic and optical studies on polyvinylpyrrolidone thin films doped with rare earth metal salts. J. Poly **42**, 728–734 (2010)
16. Abdelghany, A.M., Meikhail, M.S., Abdelrazek, E.M., Aboud, M.M.: Spectroscopic inquest of CdS, PbS and ZnS Doped PVP composite: A density functional theory approach. Res. J. Pharm. Biol. Chem. Sci. **6**, 1686–1697 (2015)
17. Soltani, N., Saion, E., Erfani, M., Rezaee, K., Bahmanrokh, G., Drummen, G.P.C., Bahrami, A., Hussein, M.Z.: Influence of the polyvinyl pyrrolidone concentration on particle Size and dpersion of ZnS nanoparticles synthesized by microwave irradiation. Int. J. Mol. Sci. **13**, 12412–12427 (2012)
18. Safo, I.A., Werheid, M., Dosche, C., Oezaslan, M.: The role of polyvinylpyrrolidone (PVP) as a capping and structure-directing agent in the formation of Pt nano-cubes. Nanoscale Adv. **1**, 3095 (2019)
19. Qian, X., Yin, J., Feng, S., Liu, S., Zhu, Z.: Preparation and characterization of polyvinylpyrrolidone films containing silver sulfide nanoparticles. J. Mater. Chem. **11**, 2504–2506 (2001)
20. Guiping, M., Dongzhi, Y., Yingshan, Z., Yu, J., Jun, N.: Preparation and characterization of chitosan/poly (vinylalcohol)/poly (vinyl pyrrolidone) electrospun fibers. Mater. Sci. **1**, 432–436 (2007)
21. Voronova, M., Rubleva, N., Kochkina, N., Afineevskii, A., Zakharov, A.: O. Surov, preparation and characterization of polyvinylpyrrolidone/cellulose nanocrystals composites. J. Nanomater. **8**, 1011 (2018)
22. Romainor, A.N.B., Chin, S.F., Pang, S.C., Bilung, L.M.: Preparation and characterization of chitosan nanoparticles-doped cellulose films with antimicrobial property. J. Nanomater **2014**, ID:710459 (2014)

23. Antonino: et.al., Preparation and characterization of chitosan obtained from Shells of Shrimp. Mar. Drugs **15**, 141 (2017)
24. Cui, L., Gao, S., Song, X., Huang, L., Dong, H., Liu, J., Chen, F., Yu, S.: Preparation and characterization of chitosan membranes. RSC Adv. **8**, 28433–28439 (2018)
25. El-Hefia, E.A., Nasefs, M.M., Yahaya, A.H.: The Preparation and characterization of chitosan /poly (vinyl Alcohol) Blended Films. E-J. Chem. **7**, 1212–1219 (2010)
26. Satija, S., Ruhi, G., Sambyal, P., Dhawan, S.K.: Synthesis and characterization of chitosan/polypyrrole nano hybrids. Frontiers of materials science in china **4**, 64–69 (2015)
27. Reddy, C.V.S., Sharma, A.K., Narasimha Rao, V.V.R.: Electrical and optical properties of a polyblend electrolyte. J. Polym. **47**, 1318–1323 (2006)
28. Abdelghany, A.M., Meikhail, M.S., El-Bana, A.A.: Characterization and amoxicillin release in novel chitosan/poly (vinyl alcohol)/sodium alginate tri-polymer matrices as restorative-spoiled wound dressings. GJP **9**, 821–831 (2019)

Figures

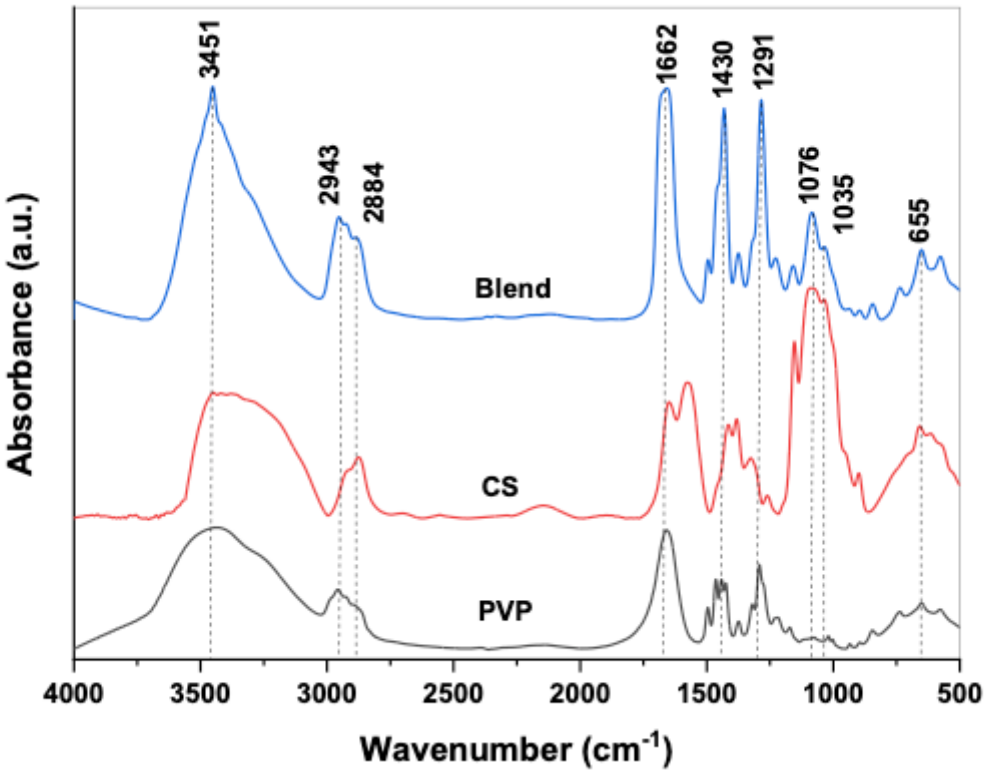

Figure 1

FT-IR absorption spectra of pure the blend, pure PVP, and pure CS.

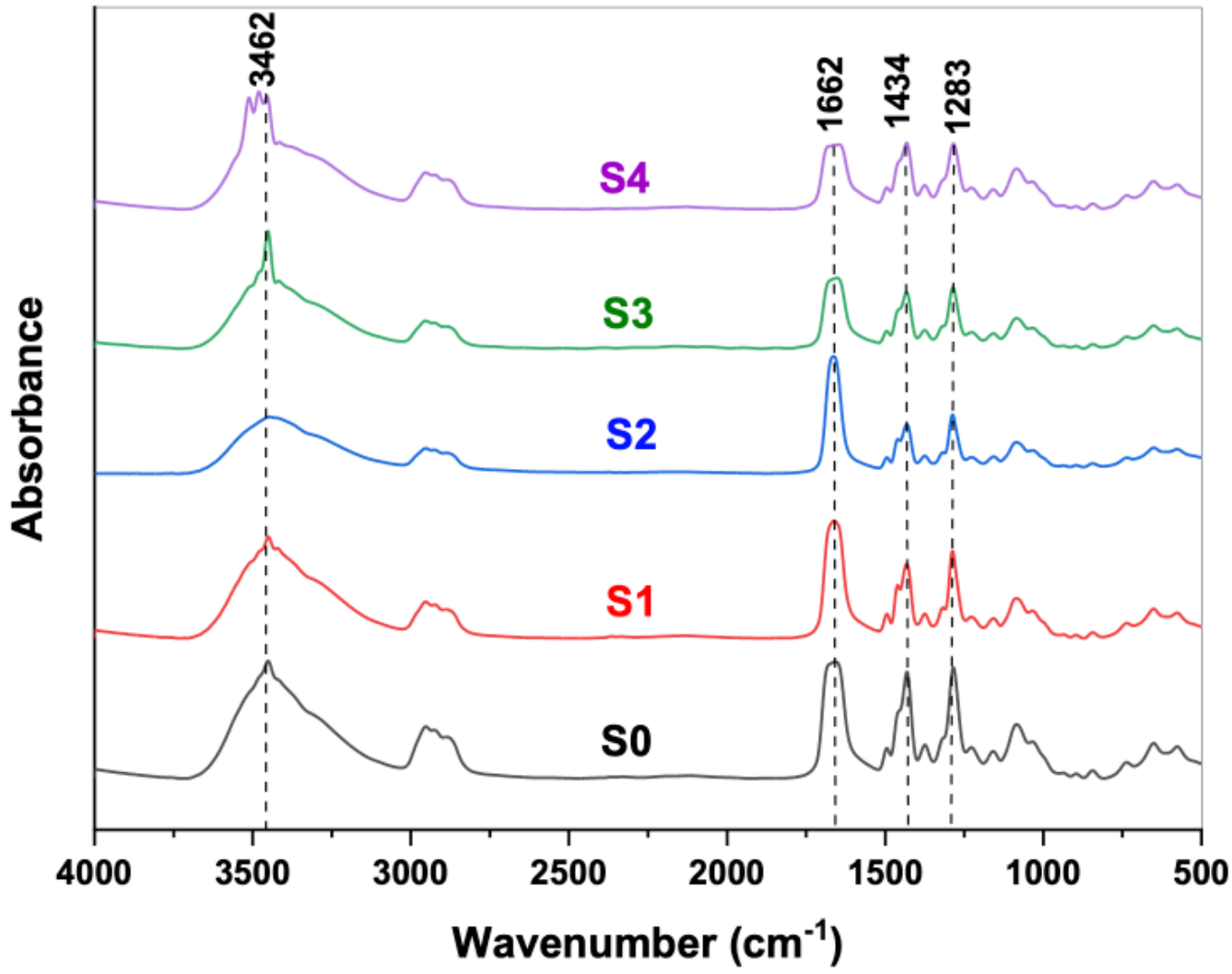

Figure 2

FT-IR absorption spectra of pure blend and biosynthesized ZnS-NPs.

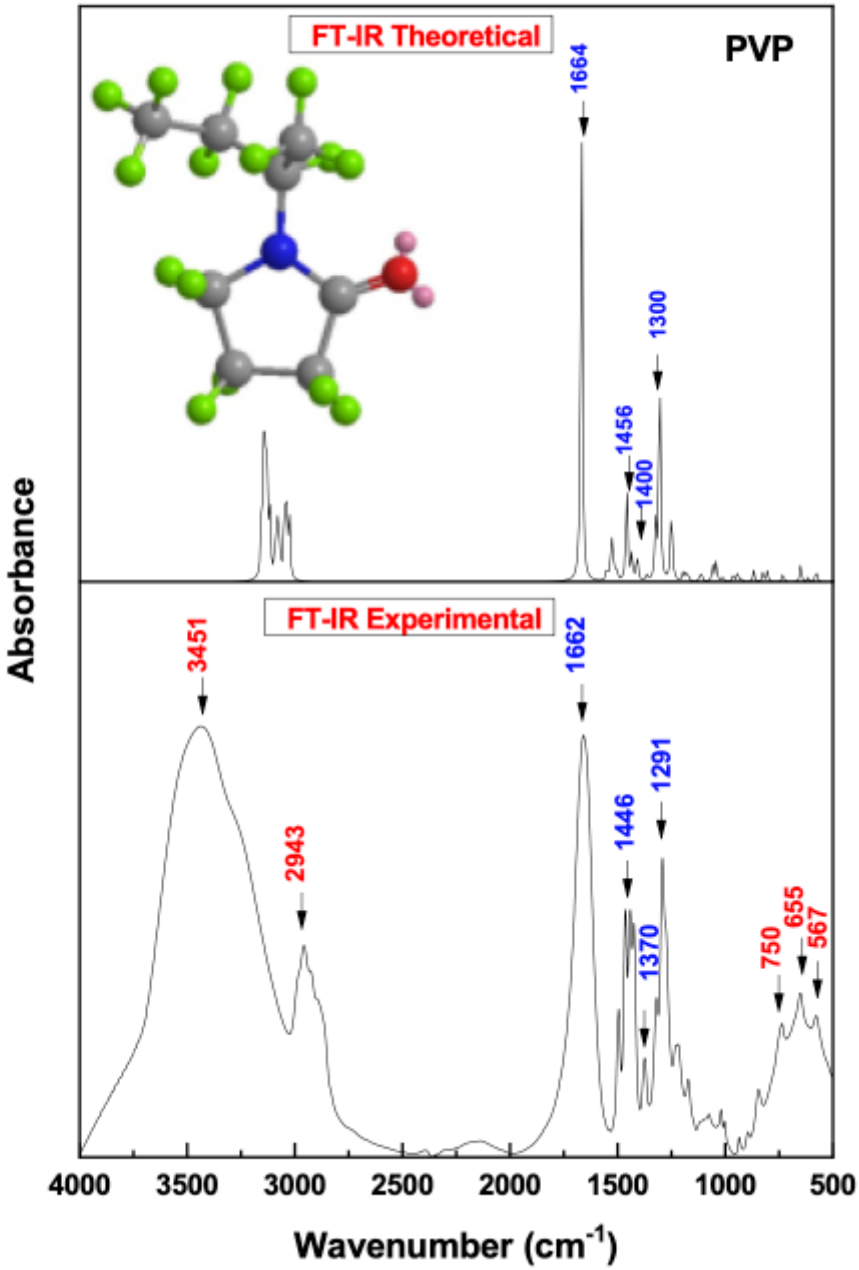

Figure 3

3D chemical structure of PVP, DFT and experiment FT-IR spectra of PVP monomer

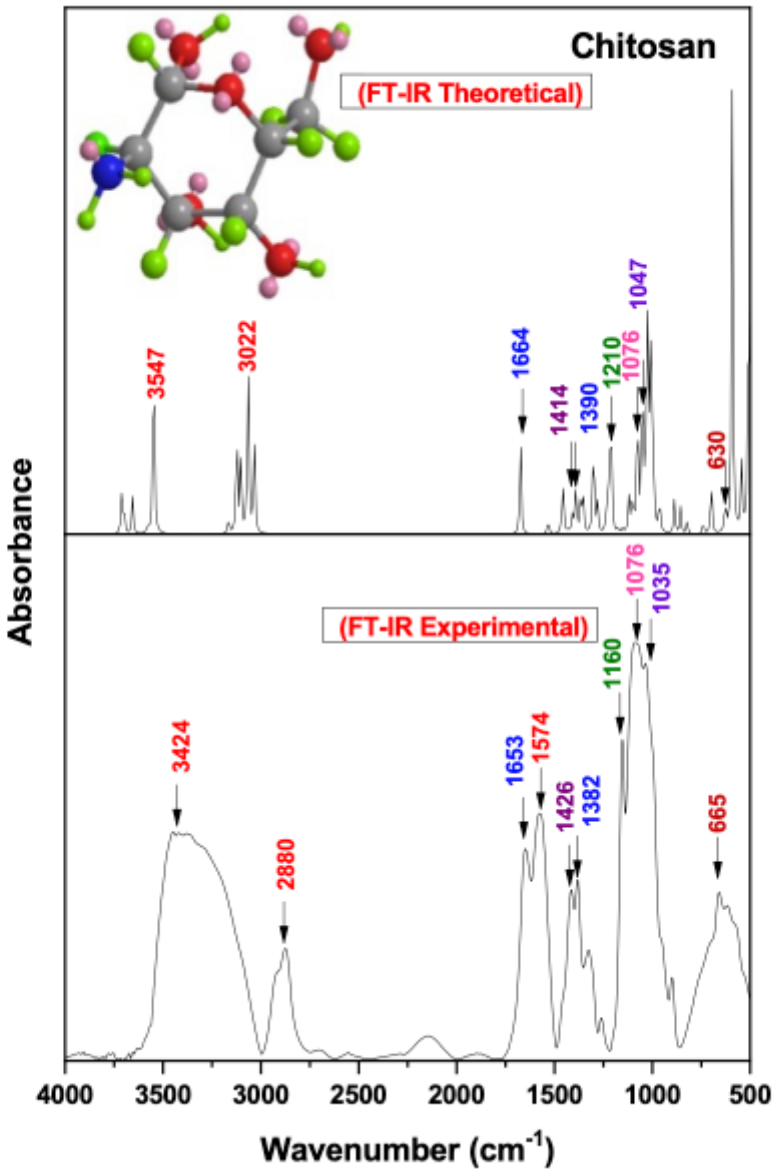

Figure 4

3D chemical structure of chitosan, experiment, and DFT FT-IR spectra of CS monomer.

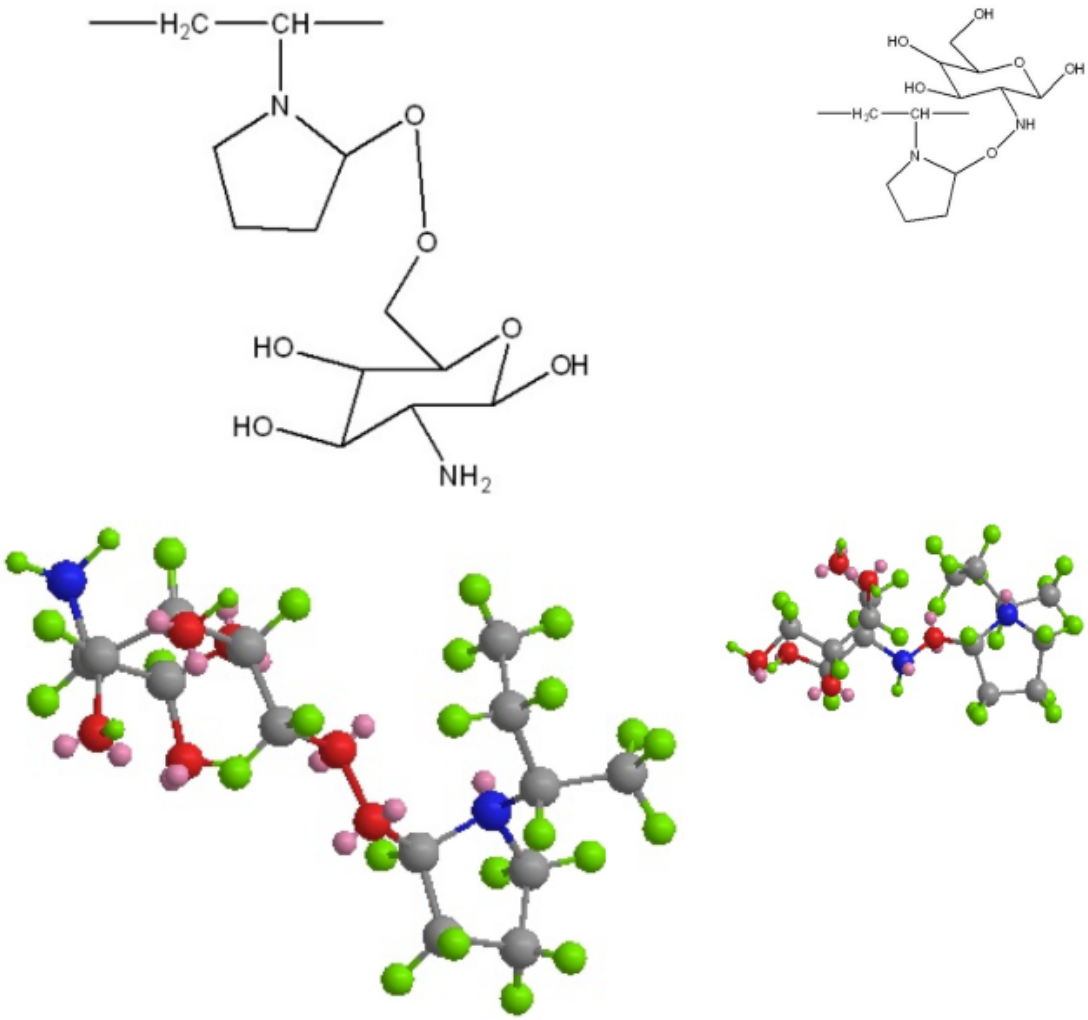

Figure 5

2D and 3D chemical structures show two different probabilities of interaction between PVP and CS, experiment and, DFT FT-IR spectra of the blend.

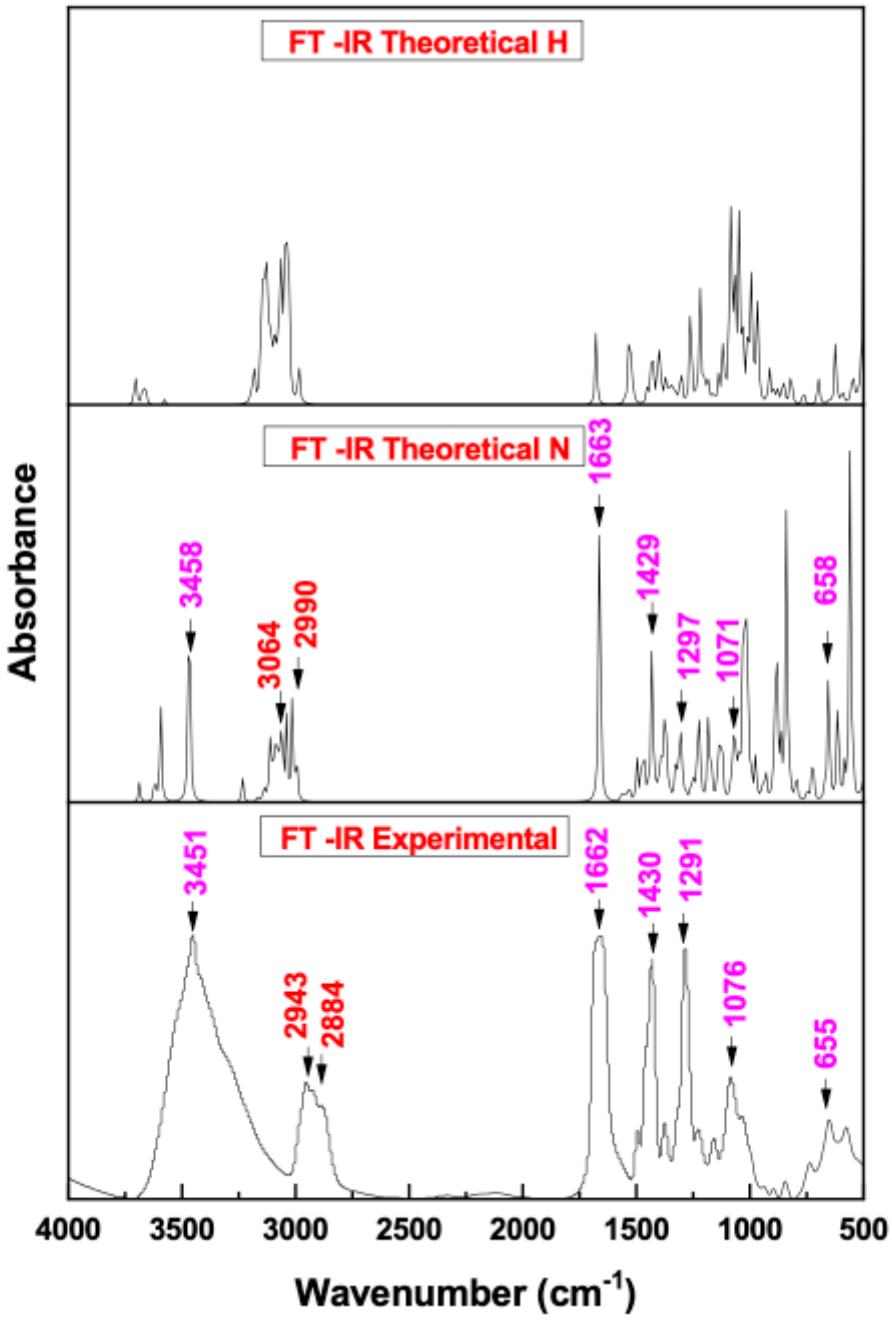

Figure 6

Experimental data of 80/20 PVP/Cs polymer blend and theoretical FTIR of the two probabilities of interaction using DFT calculations.

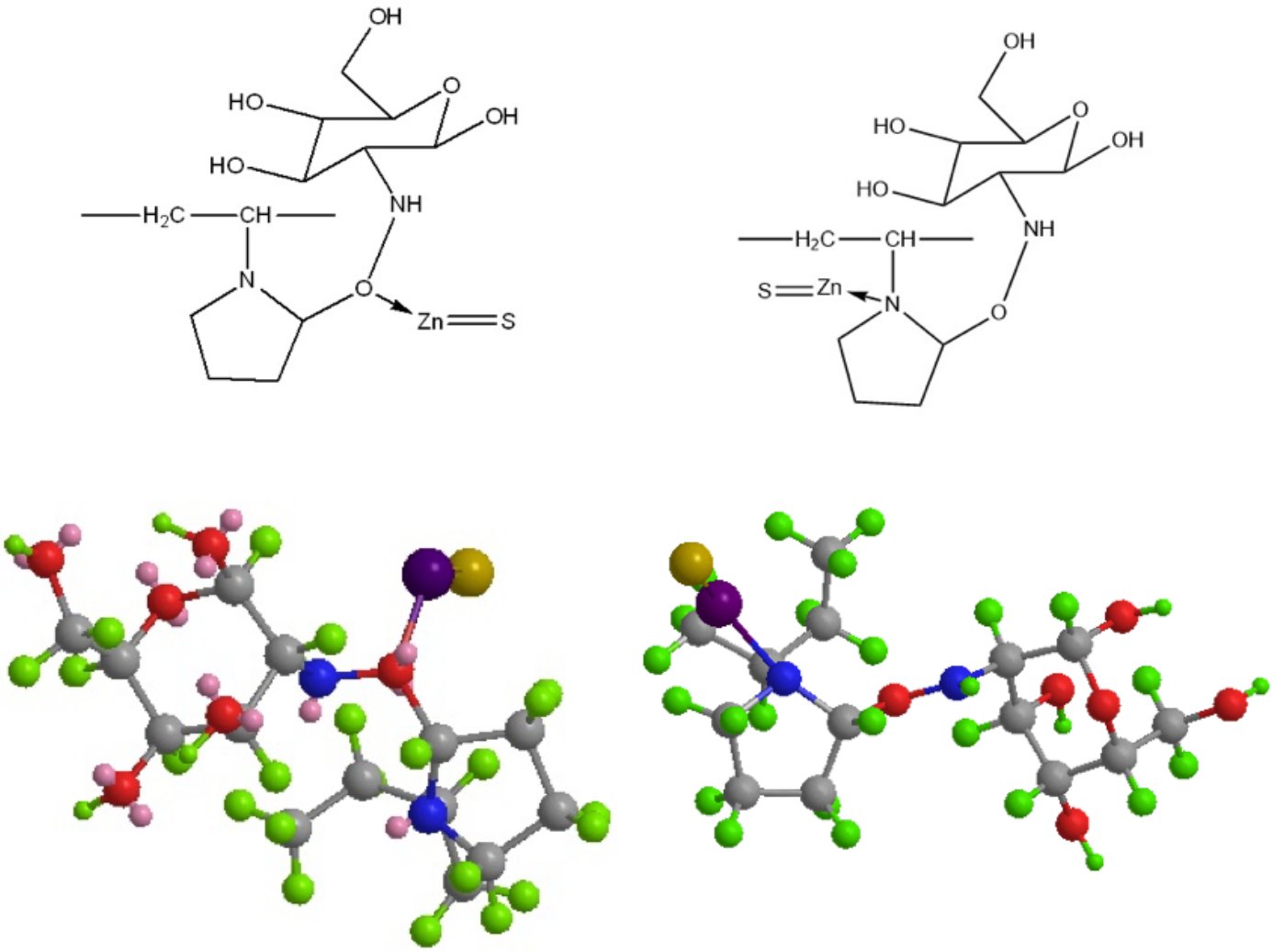

Figure 7

Graphical representation of the mechanism of interaction between the blend and ZnS-NP.

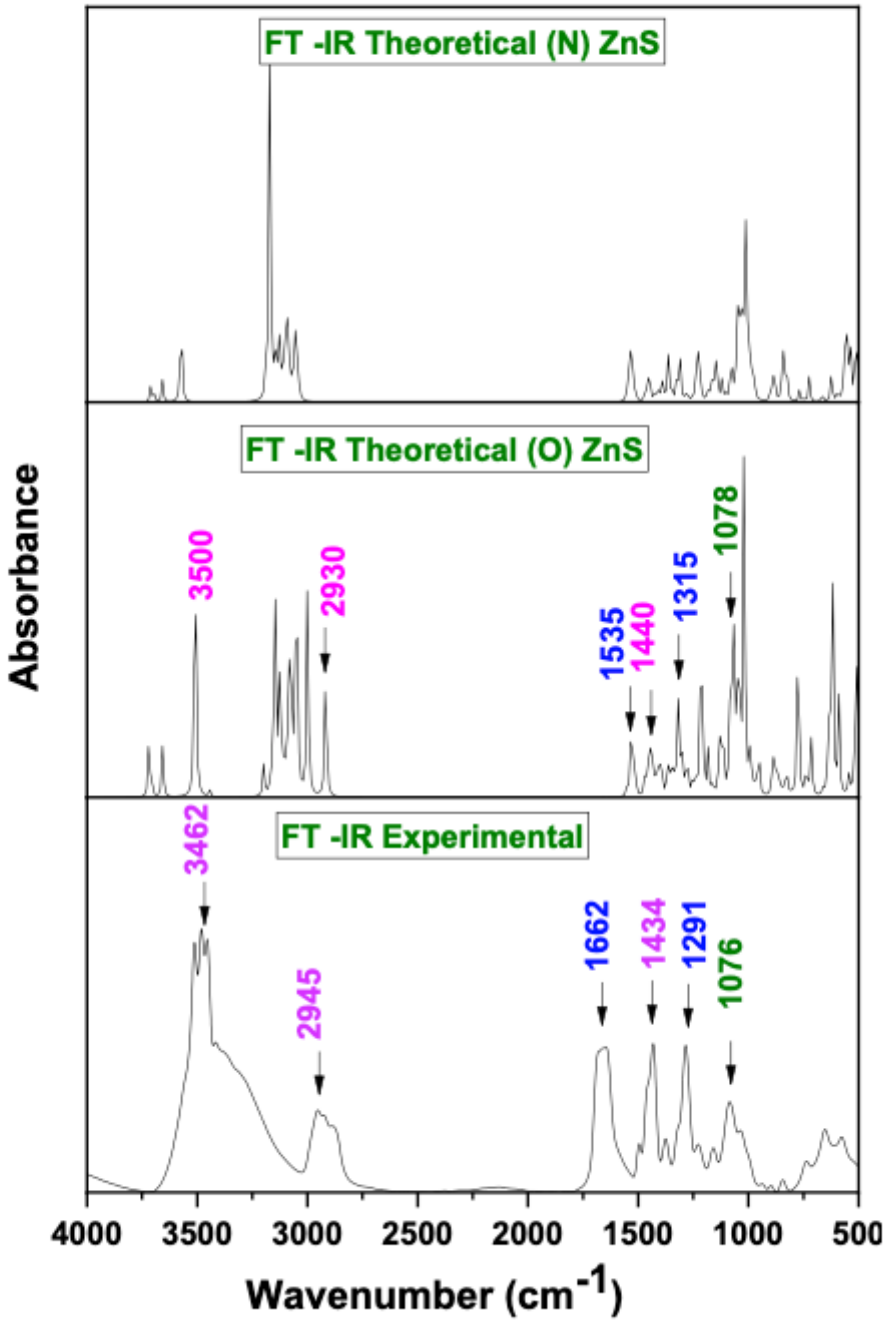

Figure 8

FT-IR Theoretical and Experimental spectra for the interaction between poly-blend and ZnS-NPs.

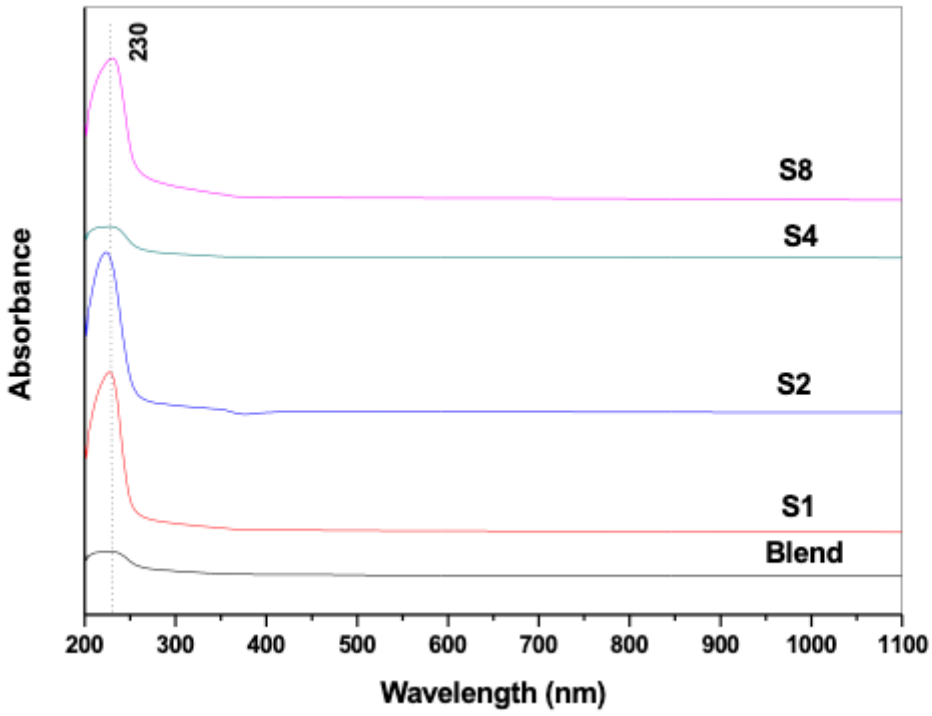

Figure 9

Spectra of UV/Vis for (PVP/CS) polymer blend doped ZnS-NPs.

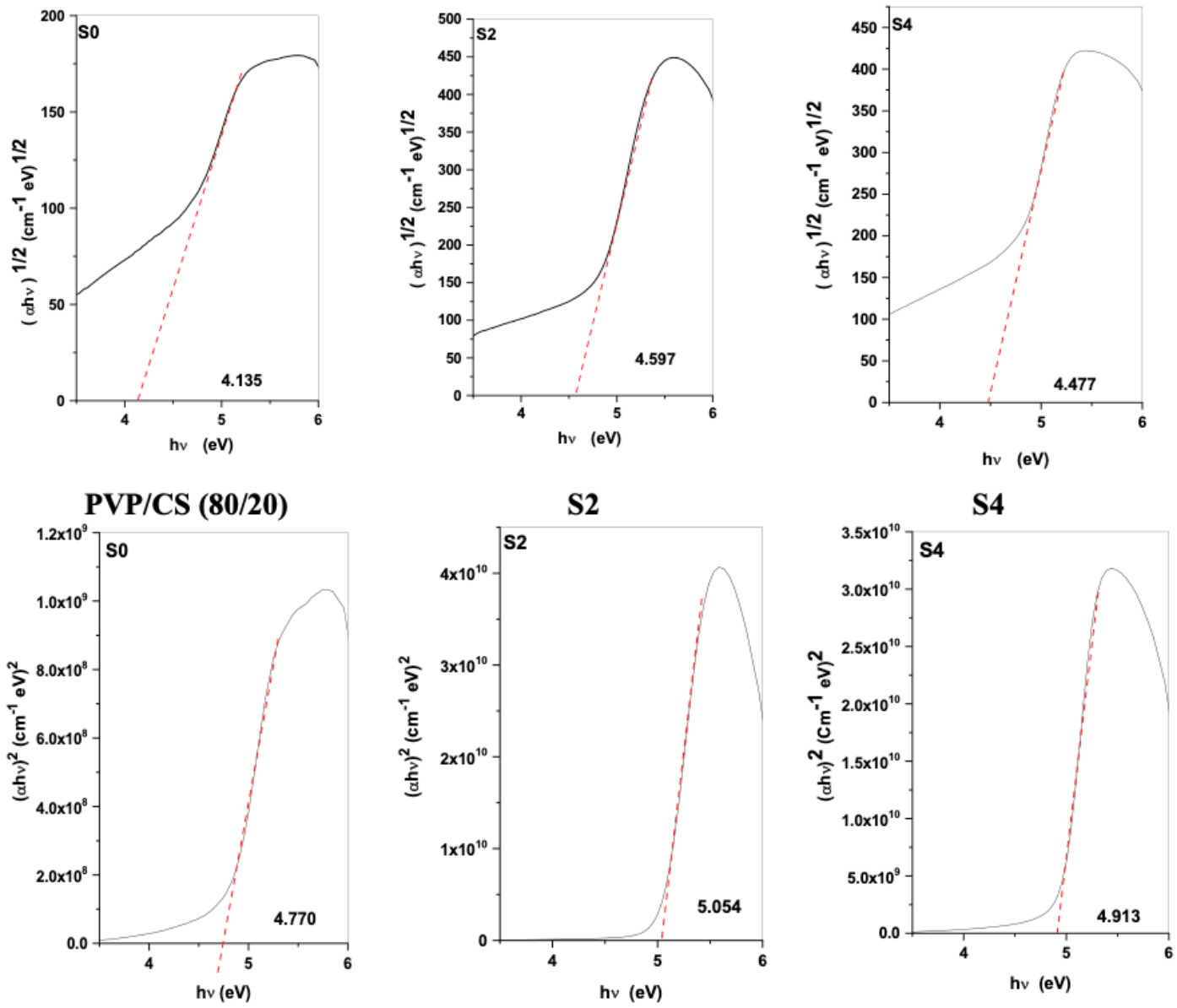

Figure 10

[(αhv)1/2 and (αhv)2] vs. photon energy (hv) for a pure blend (PVP/CS), polymer blend doped ZnS-NPs films.

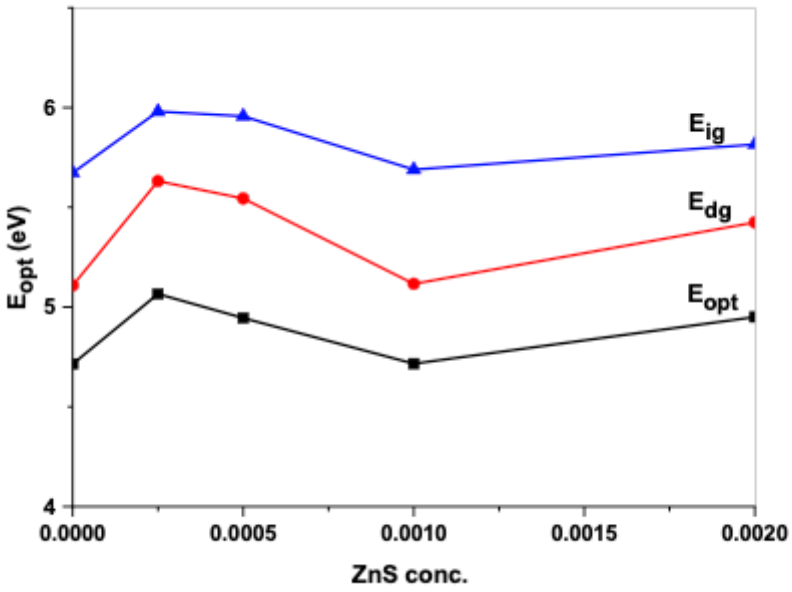

Figure 11

Direct and indirect bandgap energies as a function in ZnS concentration in the PVP/CS matrix.